Fabrication and study of characteristics of $HgSr_2$ $Ca_{n-1}Cu_nO_{\delta+10}$, (n = 1, 2 and 3) thin films superconducting

S. H. Mahdi, L. A. Mohammed, R. N. Fadhil, B. H. Hussein*
Department of physics, College of Education for Pure Science / Ibn Al-Haitham, University of Baghdad, Baghdad, Iraq

Recently, particular attention has been given to the material of Superconducting films because of its exceptional electrical and optical properties. In this work, HgSr2 Can-1CunOδ+10, (n = 1, 2 and 3) .Thin Films Superconducting have been prepared by two-step process bulk and thin film. The optical properties were calculated absorption, transmission, reflection, band gap, coefficient of absorption, excitation coefficient and index of refraction in the range of wavelengths (300-1100) nm using a double beam spectrophotometer (UV/VIS). Structural, morphological, and electrical properties were investigated using X-ray diffraction (XRD) and AFM, Using the 4-probe technique measuring the resistivity as a function of temperature. The composite HgSr2 Ca2Cu3Oδ+10 showed an improvement in all properties the structural, electrical and optical as a result of increasing of Cu-O layers.

(Received February 17, 2023; Accepted May 3, 2023)

Keywords: Superconductors, $HgSr_2Ca_{n-1}Cu_nO_{\delta+10}$, X-ray diffraction, Electrical resistivity, The optical properties

1. Introduction

A phenomenon known as superconductivity exists in two states: ideal conductivity ($\rho = 0$) and diamagnetic (χ= -1, < 1), The critical temperature, denoted by the notation (Tc), is the low temperature where this phenomena occurs with specific substances. Below a material's transition temperature Tc, superconductivity is a quantum phenomena that can occur[1-2]. The material enters the superconducting state and experiences some extraordinary macroscopic effects, including zero dc resistance and the exclusion of a magnetic field. Increasing the critical temperature to near ambient temperature is the primary goal of the majority of studies in the superconductor domain, Thus, researchers attempt to alter the conditions of preparation or exchange out certain components of compounds with others. Learn how electromagnetic and charged particle fields impact superconductivity[1-3].

Applications of superconducting are frequently employed in the engineering and medical industries. These applications are employed in laser devices that require specific operation, magnetic resonance imaging, and radiometric evaluation[1].

Kamerlingh Onnes discovered superconductivity in 1911 while testing mercury's resistance at low temperatures. The mercury Tc was found to be 4.2 °K. Since then, finding novel materials with higher critical temperatures has played a crucial role in the science of superconductivity. The element with the maximum Tc was Nb (Tc=9.2 °K), which was discovered in 1930. When binary alloys and compounds were shown to have even higher critical transition temperatures, a significant stride was taken[1-4]. The hunt for superconducting materials with high transition temperatures changed direction in 1986. At that time, Bednorz and Miiller reported on a superconducting transition for the oxide system La-Ba-Cu-O commencing at approximately 30 °K. And although oxide superconductors, such as BaPb1-xBixO3 with a maximum Tc of 11.2 °K, had been known for a very long time prior to 1986 (year of discovery 1975), The observation was completely unexpected given that oxides and other low-carrier density systems were typically thought to be poor candidates for Tc above 25 °K. The Bednorz-Miiller discovery prompted an

* Corresponding author: boshra.h.h@ihcoedu.uobaghdad.edu.iq
https://doi.org/10.15251/DJNB.2023.182.579

immediate search for nearby minerals with a higher Tc. As a result, a large family of multielemental copper oxide-based compounds with similar physical and structural characteristics was discovered. High temperature superconductors are the name given to the new materials (HTS). Several hundred HTS are known now, and some of these display superconductivity above the liquid nitrogen boiling point (77 °K), the most well-known of which exhibit zero resistance at 93 K, 110 K, and 125 K, respectively, are YBa2Cu3O7-x, Bi2Sr2Ca2Cu3O10, and T21Ba2Ca2Cu10. Of the HTS listed, YBa2Cu3O7-x is by far the most studied[1,4,5].

Hg –base superconductors are generally given by HgBa2Can-1CunO2n +2+δ (n: the number of consecutive Cu-O layers). The three phases generated using the conventional frying process are HgBa2CuO5+ (n = 1, 1201 phase, Tc = 86 °K), HgBa2CaCu2O6+ (n = 2, 1212 phase, Tc = 105 °K), and HgBa2Ca2Cu3O6+ (n = 3, 1223 phase, Tc = 132 °K)[1-2]. The production of a novel copper oxide porcelain with a higher critical temperature (Tc) of 70 Kelvin began with the synthesis of the superconducting ceramic material based on the elements of mercury, barium, copper, and oxygen[3]. The copper, strontium, calcium, and bismuth oxides used to create the unique superconducting ceramic Tc ranged in temperature from 80 to 110 °K[4]. Compounds having hole-type conductivity include numerous high-Tc cuprates and Hg-based superconductors. For example, the following process could result in the formation of holes (h)[5]:

$$O \rightarrow O^{2-} + 2h \quad (1)$$

For more than sixty years, research on thin superconducting films has been a vital part of superconductivity science. It significantly influenced how the macroscopic and microscopic nature of the superconducting state are now understood. The study of ultrathin films and surface and interface layers has become the main focus of contemporary field research. Condensed-matter physics and thin film technology have long been heavily reliant on the field of superconducting films. Superconducting films are interesting for experimental research because they can be made in ways that are challenging or impossible to achieve with pure bulk materials. A couple of examples are creating novel material structures and creating specimens whose dimensions are on the same scale as the basic superconducting characteristics[1,6]. Superconducting films are of utmost relevance in the development of small-scale electronic applications based on superconductors. These films have to meet strict specifications for their composition and electrical characteristics. Whether a complex metal oxide is superconducting or not, the setup for the manufacture of high-quality oxide thin films is typically unrelated to the physical characteristics of the oxide. High-quality superconducting cuprate synthesis is extremely difficult, especially for epitaxial thin films[1,7].

2. Experimental

The $HgSr_2Ca_nCu_{n-1}O_{2n+2+\delta}$ with (n=1, 2 and 3) high critical temperature superconducting (HTS) thin films were fabricated using two-step process (bulk and thin film). At first the precursor bulk was prepared by solid state reaction, employing the right weights of pure powders materials HgO, , SrO, CaO and CuO, and in proportion to their molecular weights. The weight of each reactant was measured by using a sensitive balance whose sensitivity is of the order (10^{-4}) gm. The powders were mixed together by using a gate mortar; a sufficient quantity of 2- propane was to homogenization the mixture and to form slurry during the process of grinding for about (40-60) minute. The mixture was put in alumina crucible and dried for an oven at 150 $^{\circ}$C. The powder was pressed into disc-shape pellets (1.5 cm) in diameter and (0.25) cm thick, using hydraulic press under a pressure of (7 ton/cm^2).The pellets were put in a furnace which has programmable controller for sintering. The pellets were sintered in air at (860) $^{\circ}$C for (24 h) with a rate of (2°C/s) and then cooled to room temperature by the same rate[3-4].

In the second step, the pellets were used as a target to prepare thin film compound on a slide glass, utilizing the DC sputtering method. Cathode voltage was in the range of 2.5 KV. The target's distance from the substrates was 4 cm. The chamber's background pressure was 10^{-4} torr. To produce the glow discharge, argon gas was injected at a pressure of around 10^{-2} torr through a

needle valve. After running the system for 4 hours, one will obtain thin film samples with thickness of 135 nm. The critical temperatures measurements were carried out using the four - point technique of the prepared specimens in a temperature from 300 down to 77 °K, and to calculate the critical temperature (Tc) by using the relation[2-4]:

$$\rho = \frac{R * A}{L} \qquad (2)$$

(Vphase) volume fraction for any phase determined by using the relation:

$$V_{ph} = \frac{\Sigma I_{\circ}}{\Sigma I_{\circ} + \Sigma I_1 + \Sigma I_2 \Sigma I_3 \Sigma I_n} \qquad (3)$$

Lattice parameter of all samples prepared have been examined using X-ray diffraction (XRD) technique using X-ray diffractometer system (SHIMADZU Japan XRD 600) by record of the intensity in the Bragg's angle range, from (10-80), Generator settings of 20 mA and 40 KV were used with a source of Cu Kα radiation with a wavelength of (=1.5405). These specimens' surface morphology as seen by the Atomic Force Microscopy (AFM) technique, by utilizing a contact mode spectrometer, SPM model AA3000, provided by Angstrom Advanced Inc. company, USA. to determine the nanocrystalline topography[2-5].

Optical properties measurements of these films grown on glass substrates were studied by recorded the transmittance (T) and absorbance (A) spectrum in the range of wavelengths (300-1100) nm using a double beam spectrophotometer (UV/VIS), to determine the optical parameters such as reflectance (R), absorption coefficient (α), optical energy gap (Egopt), refractive index (n), extinction coefficient (K), and dielectric constant (ε)[6-9].

3. Results and discussion

All results obtained have been analysed after a procedure many of tests on the specimens prepared, including the results of the diffraction X-ray (XRD), by determining the type The structure of specimens and ratios phases and lattice parameters (a, b, c) and ratio (c/a) and unit cell density. The crystallinity properties of the HgSr2 Can-1CunO+10 thin films Superconducting were examined using XRD. All specimen's were found to have polycrystalline structures with orthorhombic crystal structures, according to the results.

X-ray diffraction results revealed that specimens contained nearly pure polyphase Hg-1201, Hg-1212, Hg-1223. The X-ray diffraction pattern's d values and h, k, and l reflections were used, the lattice parameters were calculated using the least Cohen's square method. Figure(1) show series XRD patterns for $HgSr_2Ca_{n-1}Cu_nO_{2n+2+\delta}$ film where n=1,2,3 respectively from diffraction positions & peaks indicated that all the specimens have Polycrystalline structure .we see that all the specimens contain a high percentage of the high temperature phase (Hg-1223) & a few peaks of low intensity phases (Hg-1212&Hg-1201) that's has a low temperature, with appearance of some impurity phases. From comparison high phase in the all specimens, we found that there are a noticeable increment in this phase (Hg-1223) &decrement in (Hg-1212&Hg-1201&impurities) and that it can be attributed to the effect of growth in the presence of partial fusion or partial liquid phase Which works to treat defects in the microstructure such as cracks in the grains Superconductors caused by mechanical deformations during the preparation process lead to a change in the stability and the cause was the effect of preparation methods and conditions which has a great effect on oxygen concentration that's leads to

changing in phases & lattice parameters of superconductors it could also be because the increase in oxygen contact where this increase is taken by the layers of mercury that it causes stronger bonding due to the increased ionic bonding strength formed in these layers the change of factors influencing the preparation methods and conditions will cause a change in the coefficients Lattice and compaction factor (c/a)[2,6].

Table 1. The value of parameters a,,c,c/a and high ,medium and low phase HgSr2 Can-1CunO2n+n+δ (n = 1, 2 and 3)

Specimen	$a(A^0)$	$c(A^0)$	c/a	H	M	L
$HgSr_2CuO_{4+\delta}$	3.457	15.387	4.450969	74.44169	18.11414	7.444169
$HgSr_2 Ca_1Cu_2O_{6+\delta}$	3.489	15.941	4.568931	76.36364	18.18182	5.454545
$HgSr_2 Ca_2Cu_3O_{8+\delta}$	3.401	15.997	4.703617	81.48148	13.88889	4.62963

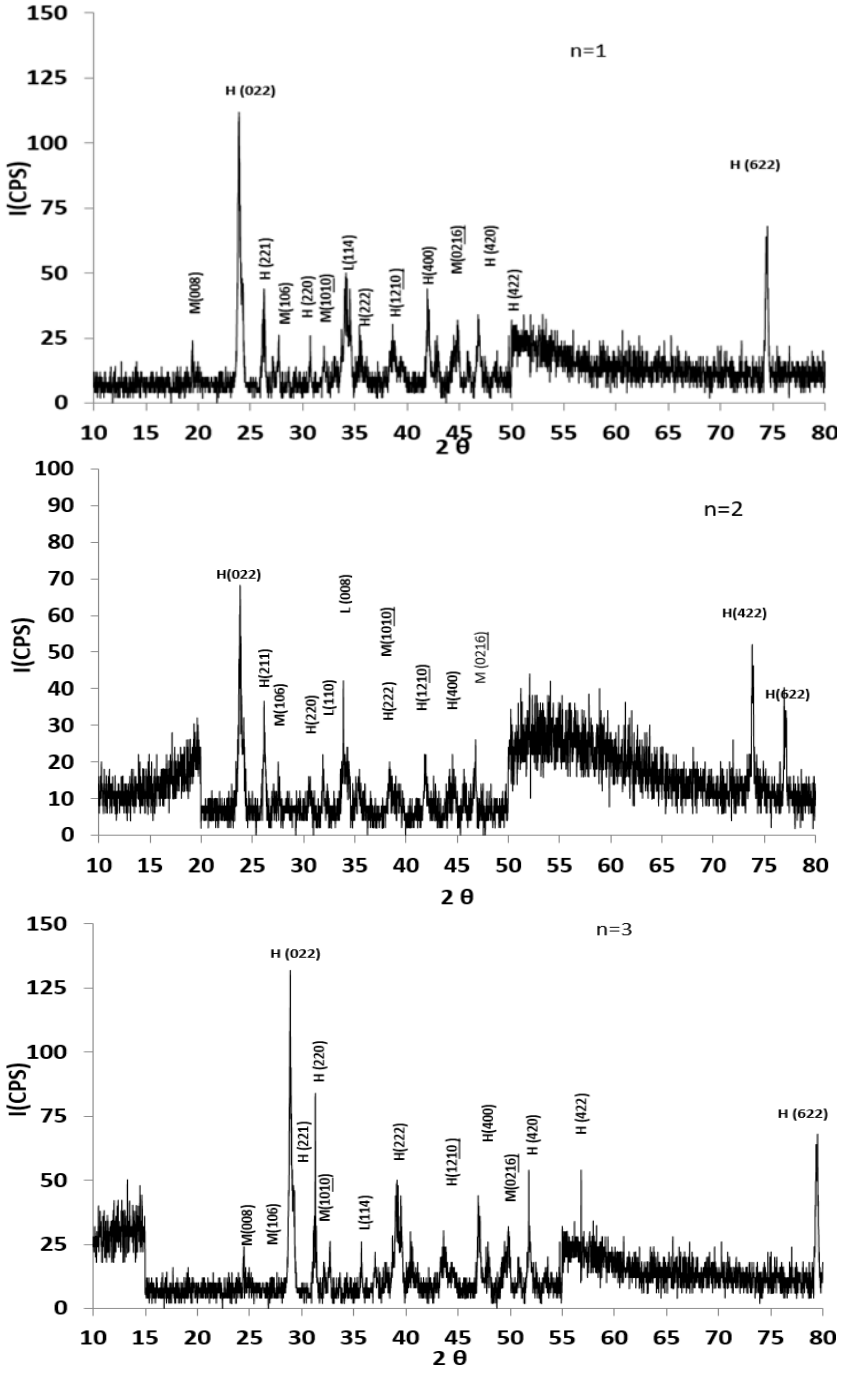

Fig. 1. XRD patterns for HgSr2 Can-1Cun Oδ+10 thin Films Superconducting with n(1,2,3).

Fig .2. displays the resistivity values vs temperature charts at n=(1,2,3) for $HgSr_2Ca_nCu_{n+\delta}$ film HTSC. Above onset temperature, which is defined as the temperature at which the resistance-temperature plot deviates from linearity, the characteristic of all spaceman was metallic, followed by a superconductivity transition with Tc =132.5°K,160°K and 158.5°K respectively[2]. While specimen with (n=3) has a higher critical temperature equal to 158.5°K, and the resistivity decreased almost sharply, the cause may be attributed to the existence of the high Tc -phase as referred to in x-ray analysis, which can be due to the significant increase in Hg-1223 and decrease in other phases (Hg-1212 and Hg-1201) when compared to other values of n because it increases Cu-O layer in 1201, 1212, and product 1223. As n values are raised, the transition width (ΔTc) narrows. This can be the result of homogeneity in the preparation of the specimen. The energy difference between the superconductor's ground state and the energy of the lowest quasiparticle excitation is known as the superconducting gap, the nature of the gap of the high temperature superconductors was revealed by a number of indicators that it maintained in the normal state at temperatures above the superconducting transition temperature. The earliest evidence for this came from NMR measurements, which discovered a gap-like depression of the density of state at the Fermi surface at a temperature T that approached Tc, close to ideal doping, but was higher than Tc at lower doping levels.

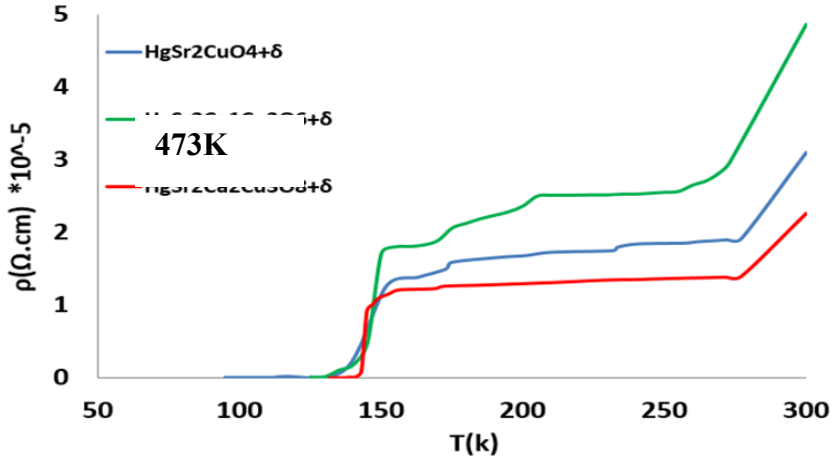

Fig. 2. The Resistivity as function of temperature for HgSr2 Can-1Cun Oδ+10 compounds n=(1,2,3)

Table 2. The transition temperature (Tcon, Tcoff) ,the transition width (ΔTc) and Energy gab Eg(eV) of HgSr2 CanCun+δ compounds n=(1,2,3)

Specimens	Tc_{on}	Tc_{off}	ΔTc	Eg(ev)
$HgSr_2CuO_{4+\delta}$	175	90	85	0.027402
$HgSr_2Ca_1Cu_2O_{6+\delta}$	205	115	90	0.035013
$HgSr_2Ca_2Cu_3O_{8+\delta}$	172	145	27	0.044147

The absorbance and transmittance spectra of (HgSr2 CanCun+δ) films can be used to estimate the optical constants. As a result, measurements of the absorbance and transmittance spectra in the wavelength range (300-1100 nm) for the produced films were made. While a UV/1800 spectrophotometer provided by the (BIOTECH) firm was used to determine the energy gap value. The Urbach law, which calculates the absorption coefficient, is expressed as follows[10-12]:

$$\alpha t = 2.303A \qquad (4A)$$

$$\alpha t = 2.303A \quad (4B)$$

where (Io, I, α, t and A) refer to the intensities of the incident, the intensities of the transmitted light, the optical absorption coefficient, the thickness of film and absorbance is defined by A= log (I_0/I) respectively . When the values of α (absorption coefficient) are high (α >104) cm-1, at higher energies, direct electronic transition will be expected and the energy and momentum conservation for the electron and photon included whereas when the values of absorption coefficient are low (α <104 cm-1) at low energies ,indirect electronic transition have been expected.

Figure (3) it demonstrates that the absorbance is greatest at wavelengths between 300 and 400 nm in the visible spectrum and close to the UV spectrum. The absorbance declines to its lowest levels in the region of near-infrared (IR) wavelengths in the region with wavelengths higher than (800 nm). Figure (4) demonstrates that as the wavelength value is increased λ > 350 nm , the transmittance value of all produced films increases.

Figure (5) demonstrates the variations of the absorption coefficient (α) versus photon energy for the thin-film superconductor HgSr2 CanCun+δ, It can be shown that all the films had large absorption coefficients(α < 104 cm-1), indicating the possibility of an indirect transition additionally, we can see that the entire spectral range exhibits an increase in absorption coefficient values as n (1, 2, 3) and photon energy increases. This effect might be caused by the films' altered crystal structure as increases n (1,2,3) for the same reasons we previously described. The Tauc equation was used to calculate the optical band gap[12-13]:

$$\alpha(h\nu) = \beta\,(h\nu - Eg)n \quad (5)$$

where β: is a constant, hν is the photon energy, Eg : is the allowed or forbidden optical energy gap for indirect and indirect transition and (n) is an exponential factor which dependent on the electronic transition, and α is the absorption coefficient. By plotting(αhν)2/3 versus photon energy(hν) the optical energy band gap of the films was determined, and by extrapolating the curve to αhν = 0[14-15].

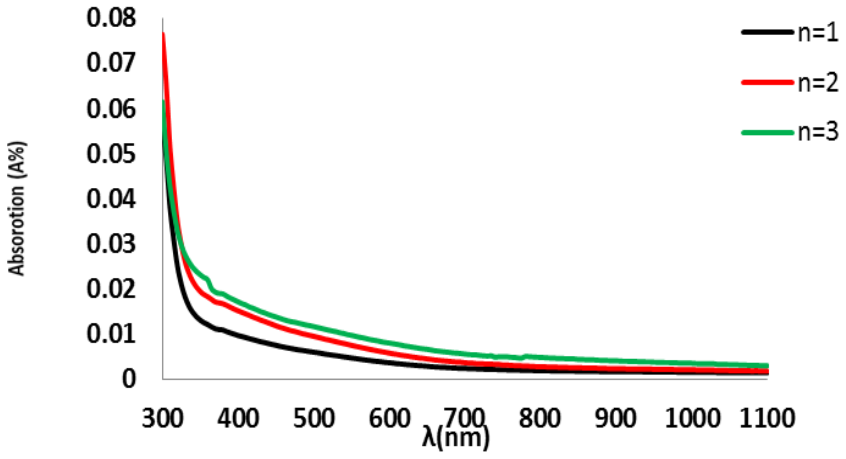

Fig. 3. Absorbance changes with Photon Energy.

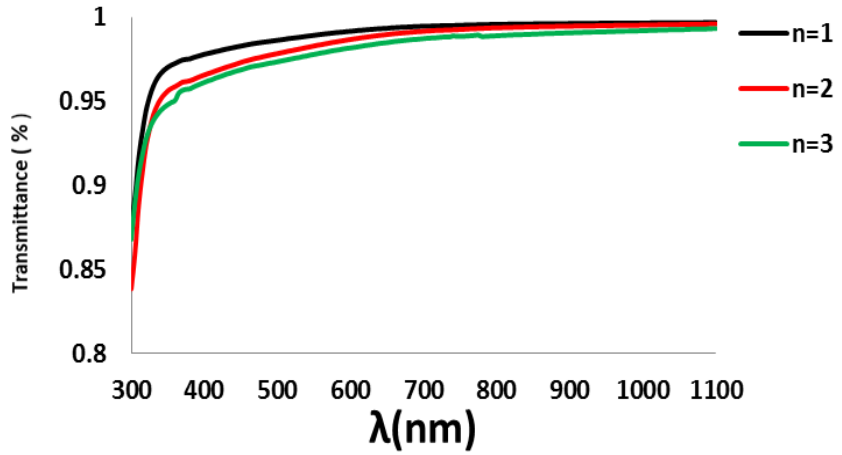

Fig. 4. The Transmittance Spectrum.

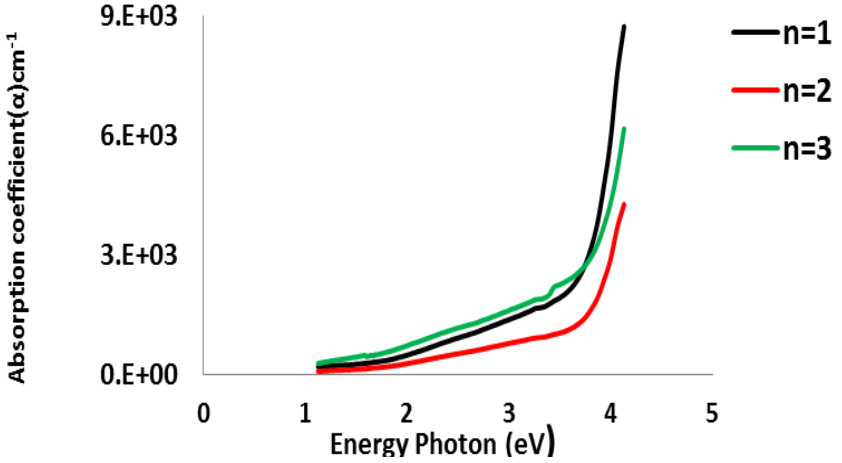

Fig. 5. Absorption coefficient of HgSr2 Ca_{n-1}Cun $O_{\delta+10}$ thin Films Superconducting with n(1,2,3).

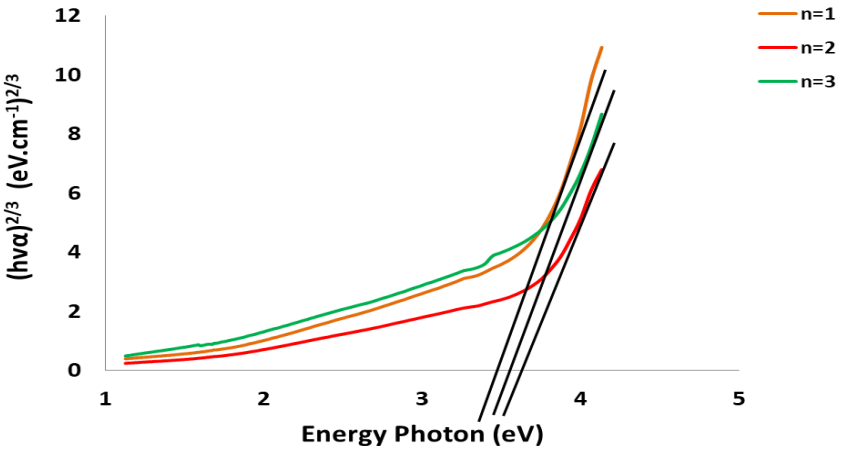

Fig. 6. Indirect allowed energy gap for(αhν)2/3 versus photon energy (hν).

Based on how a substance interacts to incident light,the refractive index n(λ) and extinction coefficient k, are an important factor of the content since They provide a general overview of the optical and dielectric specifics required for the creation of potent optical machinery for the production of solar cells and lasers[15]. The following formula is used to determine the extinction coefficient k(λ)[16-17].

$$k = \frac{\alpha \lambda}{4\pi} \quad (6)$$

when the absorption coefficient (α) and the wavelength (λ) are both represented. The average light attenuation percentage is known as the extinction coefficient (k). According to this, the highest value of k indicates that a thin layer has the maximum light attenuation. Figure (7) displays the variability in the samples' extinction coefficient k. As can be observed, the values of k rise as the energy of the incident photon rises, and they tend to reach large values for high energy photons due to the rise in absorption. Figure (8) illustrates the relationship between the incident photon energy and the change in the produced films' refractive index (n). The refractive index noticeably rises as we approach the absorption edge; hence, it reaches its greatest value at energies corresponding to the optical energy gap of the employed membrane. The rise in the frequency of indirect electronic transitions at such energies is thought to be the cause of this trend.

The following two equations are used to calculate the complex dielectric constant of the medium ($\varepsilon_{complex}$), which is described as partial real and imaginary:

$$\varepsilon_r = n^2 - k^2 \quad (7)$$

$$\varepsilon_i = 2nk \quad (8)$$

The figure (9) shows the behavior of the dielectric constant in its real part (ε_r) as a function of the energy of the photon falling on the prepared films, and we notice that the real dielectric constant starts to increase gradually until it reaches its maximum value near the energy gap. The real dielectric constant depends on both the refractive index and the quenching coefficient, but because the quenching coefficient is less than the values of the refractive index, it depends primarily on the refractive index. It is also noted that there is a similarity between the real dielectric constant curve and the refractive index curve because the relationship between them is direct**.**

The figure (10) demonstrates that the imaginary dielectric constant(ε_i) has lower values than the real dielectric constant, indicating that ($\varepsilon_r > \varepsilon$) the imaginary dielectric constant measures how much radiation energy is absorbed by the material's atoms, and that its concept is connected to the extinction coefficient.

After measuring the value of the membranes resistance (ρ) for each temperature, the continuous electrical conductivity($\boldsymbol{\sigma_{dc}}$)was computed to analyze the nature of the conduction mechanism of the produced films[11]. The continuous conductivity was then derived using equation (9)

$$\sigma_{dc} = \frac{1}{\rho} \quad (\Omega.cm)^{-1} \quad (9)$$

Using the following equations, the Hall coefficient (R_H), carrier concentration (N), and Hall mobility (H) were all calculated:

$$R_H = \frac{-1}{qp} \ , \ (\frac{cm^3}{C}) \quad (7)$$

$$n = -\frac{1}{q} R_H, \ (\frac{1}{cm^3}) \quad (8)$$

$$\mu_H = |R_H| \ \sigma \quad (9)$$

From the negative values of the Hall coefficients for thin films of HgSr2 $Ca_{n-1}Cu_n$ $O_{\delta+10}$ Superconducting with n(1,2,3) the prepared specimens' n-type conductivity this result is consistent with references[18-20].

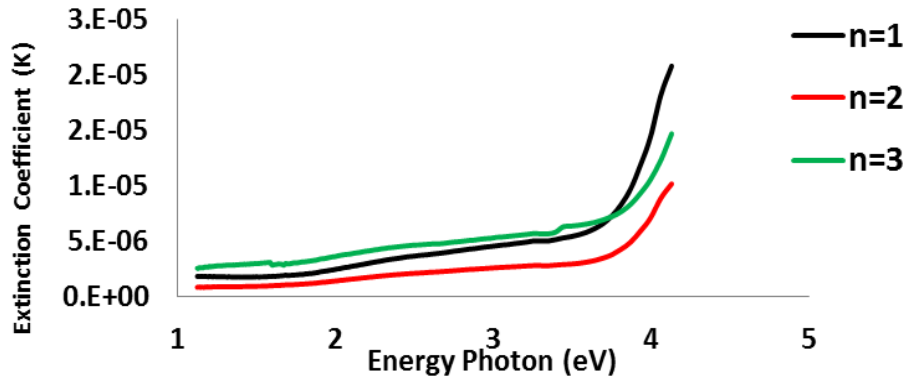

Fig. 7. Variation of the extinction coefficient of HgSr2 Can-1Cun Oδ+10 thin Films Superconducting with n(1,2,3)

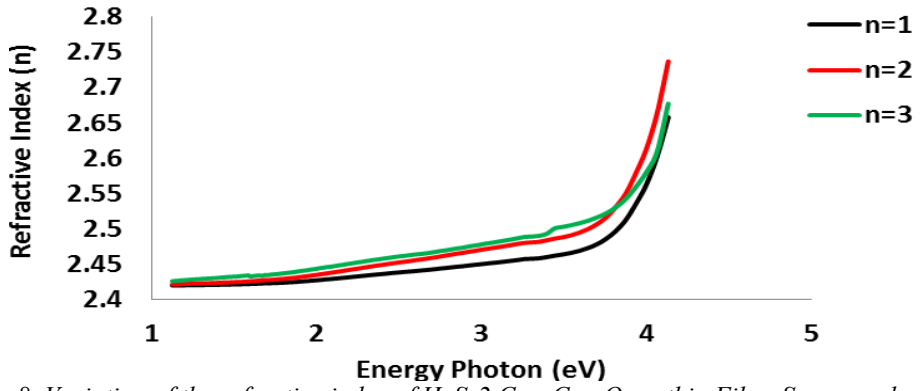

Fig. 8. Variation of the refractive index of HgSr2 Ca_{n-1}Cun $O_{\delta+10}$ thin Films Superconducting with n(1,2,3)

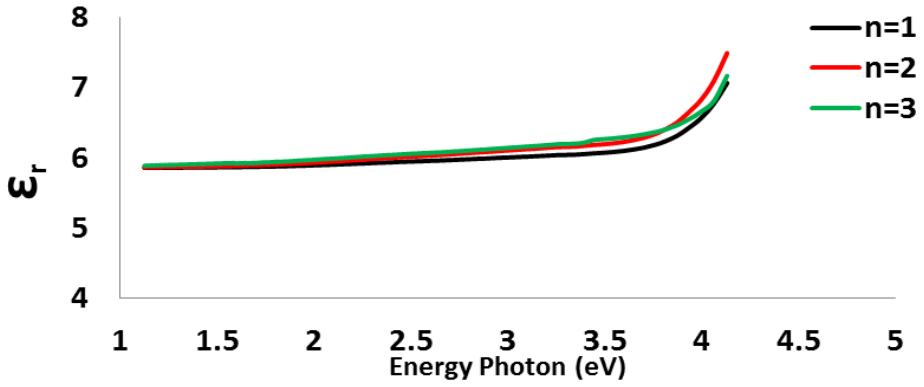

Fig. 9. The Real part (ε_r) as a function of the energy of the photon.

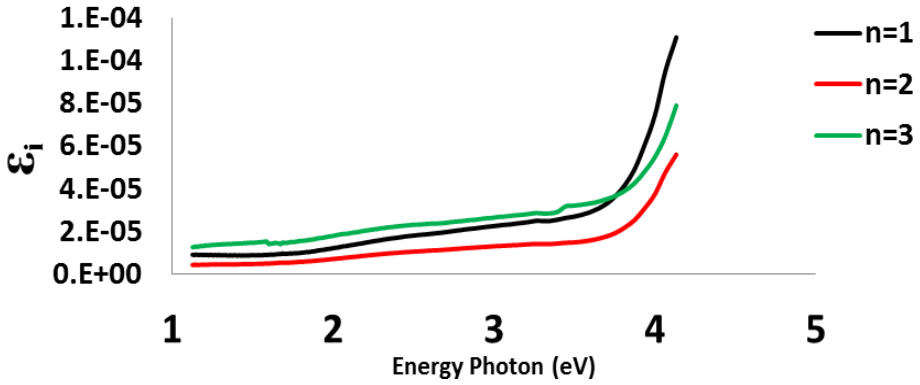

Fig.10. The imaginary dielectric constant as a function of the energy of the photon.

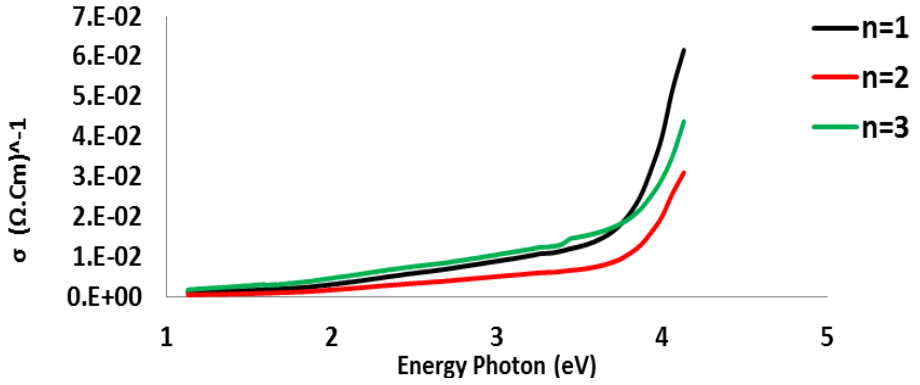

Fig. 11. The Electrical Conductivity of HgSr2 Can-1Cun Oδ+10 thin Films Superconducting with n=1,2,3.

The atomic force microscope (AFM) technology, which has a high analytical capacity of (0.1-1.0) nm and a magnification power of approximately to (3 x 10^9) times, was employed to expand the image of the thin film's surface. AFM processing is a surface characterization technique that can be used to examine the surface morphology of these films. The following pictures illustrate the analysis of the surface topography of the prepared films and the impact of adding more Cu layers using atomic force microscopy (AFM):

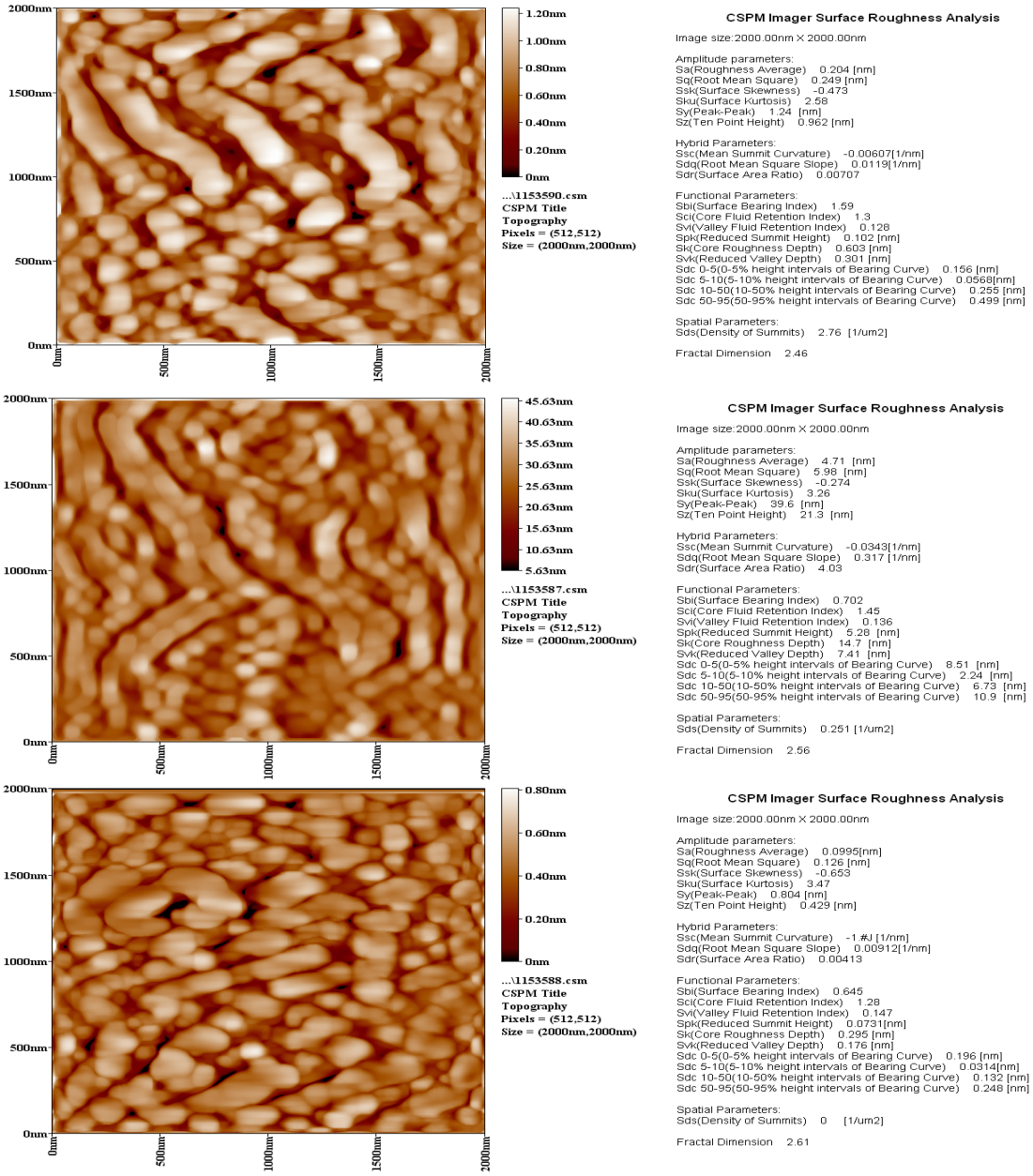

Fig. 12. 2D AFM images of HgSr2 Can-1Cun Oδ+10 thin Films Superconducting with n(1,2,3).

4. Conclusions

In summary, HgSr2 Can-1Cun Oδ+10 superconducting thin films with different n (1,2,3) were elaborated prepared by two-step process bulk and thin film. To more accurately evaluate the effects of the (n) on HgSr2 Can-1Cun O+10 superconducting thin films on the basis of their morphological, optical, and structural properties, We employed various characterization techniques identification of thin film structures, carried out using X-ray diffraction we noticed an improvement in the structural properties at a value of n = 3 as well as an increase in the higher phase Vph (1223). The band gap values of the HgSr2 Can-1Cun Oδ+10 superconducting thin films were determined by the optical examination. increasing from 0.027402 eV to 0.035013 eV to 0.044147eV for n=1,2,3 respectively.

References

[1] M.A. Omar, Elementary solid state physics, 5th ed., Addision - Wesley, (1993)

[2] K A Jasim and L A Mohammed, Journal of Physics: Conference Series, 1003, (2018).

[3] Laheeb A. Mohammed, Kareem A. Jasim, Energy Procedia 157(2019) 135-142; https://doi.org/10.1016/j.egypro.2018.11.173

[4] K.A.Jassim,H.S.hussein, Ibn Alhaitham Journal for pure and Applied Science,Vol.30,Issue3,2017; https://doi.org/10.30526/30.3.1600

[5] Laheeb A. Mohammed, Kareem A. Jasim, Ibn Al-Haitham Jour. for Pure & Appl. Sci. ,Vol. 31 (3) 2018; https://doi.org/10.30526/31.3.2024

[6] Kareem. A. Jasim, Journal of superconductivity and novel magnetism , Volume 25, Issue 6 ,Page 1713-1717, (2012); https://doi.org/10.1007/s10948-012-1507-3

[7] K. Jung-Min and K. Myung-Ho, International Journal of Technology and Engineering Studies, 2(4), 117-124, (2016).

[8] D Fonnesu, A Baris , S Calatroni, L Lain Amador, S Pfeiffer , G Rosaz, M Bonura and C Senatore, Supercond. Sci. Technol. 35 (2022) 125003 (11pp); https://doi.org/10.1088/1361-6668/ac9c99

[9] Razeg KH, Al-Hilli MF, Khalefa AA, Aadim KA, International Journal of Physics 2017; 5(2): 46-52.

[10] Eason, R. (Ed.). (2007), Pulsed laser deposition of thin films: applications-led growth of functional materials. John Wiley & Sons; https://doi.org/10.1002/0470052120

[11] David Sibanda, Sunday Temitope Oyinbo, Tien-Chien Jenand Ayotunde Idris Ibitoye, Processes 2022, 10, 1184; https://doi.org/10.3390/pr10061184

[12] Rana Hameed Athab, Bushra H. Hussein, Journal for Pure and Applied Sciences, 35(4)2022; https://doi.org/10.30526/35.4.2868

[13] Esraa A. Abbas, Ibn Al-Haitham Journal for Pure and Applied Sciences, 33 (2) 2020; https://doi.org/10.30526/33.2.2438

[14] Simon A. Bretschneider, Jonas Weickert, James A. Dorman, and Lukas Schmidt-Mende, APL Materials ; 2 , 040701, pp:1-9, (2014); https://doi.org/10.1063/1.4871795

[15] Miguel Anaya , Gabriel Lozano, Mauricio E. Calvo , Wei Zhang , Michael B. Johnston, Henry J. Snaith, and Hernan Míguez , J. Phys. Chem. Lett. 2015, 6, 48−53,(2015); https://doi.org/10.1021/jz502351s

[16] Ghada Bousselmi a, Naoufel Khemiri a, Mounir Kanzari, Optical Materials 134 (2022) 113187; https://doi.org/10.1016/j.optmat.2022.113187

[17] R. H. Athab, B. H. Hussein, Digest Journal of Nanomaterials and Biostructures, Vol. 17, No. 4, 2022, p. 1173-1180; https://doi.org/10.15251/DJNB.2022.174.1173

[18] D. Poelman, P.F. Smet, J. Phys. D Appl. Phys. 36 (2003) 1850-1857; https://doi.org/10.1088/0022-3727/36/15/316

[19] S. N. Sobhi, B. H. Hussein, Effect of annealing on thin film AgInSe2 solar cell, Journal of Ovonic Research, Vol. 18, No. 4, 2022, p. 519 – 526; https://doi.org/10.15251/JOR.2022.184.519

[20] Yu Yang, Shu Jin, Julia E. Medvedeva, John R. Ireland, Andrew W. Metz, Jun Ni, Mark C. Hersam, Arthur J. Freeman, Tobin J. Marks, J. Am. Chem. Soc. 127, 8796 (2005); https://doi.org/10.1021/ja051272a